

## Electron-Capture Cross Sections for Protons Passing through Hydrogen Gas

F. L. RIBE

*Department of Physics and Institute for Nuclear Studies, University of Chicago, Chicago, Illinois*

(Received June 4, 1951)

Measurements have been made of the electron-capture cross sections  $\sigma_e$  in hydrogen gas for protons moving with kinetic energies between 34 and 149 kev. At these energy limits,  $\sigma_e$  has the values  $1.52 \times 10^{-18}$  and  $2.29 \times 10^{-18}$  cm<sup>2</sup>, respectively. Using the values of the electron-loss cross sections  $\sigma_l$  for hydrogen atoms in hydrogen gas recently measured in this laboratory, the ratio  $\sigma_l/\sigma_e$  was derived from the results of the present measurements. Direct measurements of this ratio agreed with the values derived from the separate measurements of  $\sigma_l$  and  $\sigma_e$  to within 10 percent.

In the present case  $\sigma_l/\sigma_e$  is unity at an ion velocity of 1.44 Bohr units ( $e^2/\hbar$ ). This may be compared with the traversal of metals by protons, for which  $\sigma_l/\sigma_e=1$  is attained at 0.95 Bohr unit.

### I. INTRODUCTION

THE processes by which ions capture and lose electrons in passing through matter were the subject of many early investigations using low energy canal rays and the high energy alpha-particles from radioactive sources.<sup>1</sup> Recent measurements by Hall,<sup>2</sup> on the ratio of loss and capture cross sections for protons in various metals, and by Montague,<sup>3</sup> on the loss cross sections for hydrogen atoms in hydrogen gas have extended these studies to intermediate energies (35 to 400 kev).

Rudnick<sup>4</sup> and Bartels,<sup>5</sup> in their low energy work on ions in gases, made use of the fact that an initially charged beam acquires a neutral component as the gas is introduced into its path, until at sufficiently high densities there occurs an equilibrium distribution of neutral and charged particles which is unchanged by further increases in gas pressure. The ratio of the charged to the neutral component of the beam, after it had passed through a gas chamber, gave a measure of the ratio of loss and capture cross sections. From this measurement and a measurement of the variation of the charged-to-neutral ratio with gas pressure, before equilibrium, the capture and loss cross sections could be obtained. Meyer<sup>6</sup> has also used this method at higher energies, obtaining, among his results, three measurements of the capture cross sections for protons in hydrogen gas at energies between 35 and 145 kev.

In the work of Montague<sup>3</sup> a direct measurement was made of the loss cross section without using the equilibrium ratios as an intermediate step. By causing the moving neutral atoms to be deflected out of the beam immediately upon becoming charged, an exponential decay of the neutral-beam intensity with gas pressure

was obtained, from which the cross sections were determined.

Goldmann,<sup>7</sup> Rostagni,<sup>8</sup> Wolf,<sup>9</sup> and, more recently, Keene,<sup>10</sup> using low energy ions, have determined capture cross sections by using a known current of ions and measuring the positive-ion current arising in a known path length from the stripped gas atoms as a function of pressure. Smith<sup>11</sup> measured capture cross sections in the same energy range by observing the exponential decrease in ion-beam current at three positions along the path of the ions in the gas, assuming that only capture events occurred at the pressures used. Bartels<sup>5</sup> also applied this principle, obtaining values of the capture cross sections for protons in hydrogen in good agreement with those measured by the equilibrium method.

In the present experiment the capture cross sections for protons in hydrogen gas in the intermediate range of energies were obtained by a method similar to that used by Montague for the loss cross sections. A beam of protons entered an evacuated chamber, sealed from the beam-defining tube by a thin window. Traversing the chamber was a magnetic field which bent the proton orbits along a circular path which ended in a faraday cage. As hydrogen gas at low pressure was introduced into the chamber, some of the protons captured orbital electrons from the gas molecules, thus becoming neutral; they then moved off tangentially to the circular path, missing the faraday cage. Using Montague's notation, the ratio of the number  $N(p)$  of protons in the attenuated beam corresponding to gas pressure  $p$ , to the number  $N(0)$  of protons entering the faraday cage when the chamber was evacuated, is

$$\rho(p) \equiv N(p)/N(0) = \exp[-n(p)\sigma_e d], \quad (1)$$

where  $n(p)$  is the number of atoms per cubic centimeter of the gas,  $d$  is the length of the circular path from entrance window to detector, and  $\sigma_e$  is the electron-capture cross section per atom of hydrogen for protons

<sup>1</sup> E. R uchardt, *Hand. Physik* **XXII/2**, 103 (1933). This article contains a review of the subject and a summary of the older results. Further references are contained in the papers of Hall and Montague (references 2 and 3, below).

<sup>2</sup> T. Hall, *Phys. Rev.* **79**, 504 (1950).

<sup>3</sup> J. H. Montague, *Phys. Rev.* **81**, 1026 (1951).

<sup>4</sup> P. Rudnick, *Phys. Rev.* **38**, 1342 (1931).

<sup>5</sup> H. Bartels, *Ann. Physik* **6**, 957 (1930); **13**, 373 (1932). The latter reference contains the results for protons in hydrogen gas.

<sup>6</sup> H. Meyer, *Ann. Physik* **30**, 635 (1937).

<sup>7</sup> F. Goldmann, *Ann. Physik* **10**, 460 (1931).

<sup>8</sup> A. Rostagni, *Nuovo cimento* **15**, 117 (1939).

<sup>9</sup> F. Wolf, *Z. Physik* **74**, 575 (1932).

<sup>10</sup> J. P. Keene, *Phil. Mag.* **40**, 369 (1949).

<sup>11</sup> R. A. Smith, *Proc. Cambridge Phil. Soc.* **30**, 514 (1934).

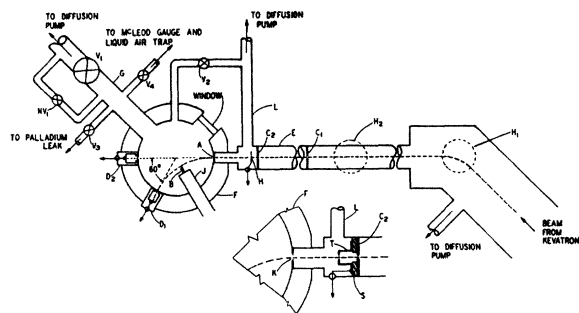


Fig. 1. Apparatus, schematic.

of the energy under consideration. In the following  $\rho(p)$  will be called the "attenuation ratio."

In applying capture and loss information to the calculation of the energy loss by moving ions at intermediate energies, the ratio of loss and capture cross sections is of primary interest. This ratio, as a function of energy, can now be obtained by dividing the loss cross sections measured by Montague by the capture cross sections of this experiment.

The consistency of the separate measurements of loss and of capture cross sections was checked at a few energies by means of an equilibrium method similar to that employed by Bartels and others. Using no magnetic field, a well-defined beam of protons was directed from the entrance aperture straight across the chamber to a faraday cage (which would not register neutral particles). As gas was admitted, some of the original protons became neutralized, and the proton current to the cage decreased to an equilibrium value. If  $\sigma_l/\sigma_c$  is the ratio of loss and capture cross sections, and the incident beam is composed entirely of protons, equilibrium value of  $\rho(p)$  is given by

$$\rho_e = (\sigma_l/\sigma_c)/(1 + \sigma_l/\sigma_c). \quad (2)$$

Thus the measured values of  $\rho_e$  could be compared with those calculated from the values of  $\sigma_c$  and  $\sigma_e$  at corresponding energies.

## II. APPARATUS

Figure 1 is a schematic diagram of the apparatus, the main components of which were the beam-defining tube *E*, the electron-exchange chamber *F*, and the vacuum manifold *G*. This diagram will be referred to throughout this section.

### A. Experimental Arrangement for Measuring the Capture Cross Sections

#### 1. The Beam-Defining Apparatus

The beam of protons was provided by the University of Chicago 400-keV Cockcroft-Walton accelerator, or kevatron. After either the atomic or the molecular component was selected by the analyzing magnetic field  $H_1$ , the beam entered the beam-defining tube *E*

with diaphragms  $C_1$  and  $C_2$  (hole diameter=0.158 cm, spacing=86 cm). The beam then passed through a monitoring screen *H* and entered the electron-exchange chamber *F* through a thin aluminized zapon window *A* which provided a vacuum seal between the exchange chamber and the beam-defining tube. For the range of energies used in this experiment the windows had an average thickness of 6.2 kev. A weak magnetic field  $H_2$  provided fine adjustment of the beam position in the horizontal plane.

It was necessary to shield the beam from the stray magnetic field during its passage through tube *E*; hence, the tube itself was made of steel and was surrounded by an outer steel tube to a distance of 71 cm from the exchange chamber. Additional magnetic shielding was placed around the beam-defining tube to a distance of 22 cm from the exchange chamber.

#### 2. The Electron-Exchange Chamber

This chamber, as well as the monitoring screen *H* and the current-measuring amplifiers, has been described in some detail in Montague's paper.<sup>12</sup> It had an inside diameter of 12.70 cm and an over-all (outer) height of 3.17 cm. An axial magnetic field was provided by an electromagnet between whose pole faces the chamber fitted snugly. The inside diameter of the chamber and that of the poles was the same, so that the slits of detectors  $D_1$  and  $D_2$ , as well as window *A*, lay directly between the circular edges of the pole faces.

The bent beam, indicated by the dashed circular line, entered detector  $D_1$ , after being deflected by 60 degrees, through a 1.06-mm slit defined by a pair of knife edges and was collected by a faraday cage. After amplification, the current to the detector (and similarly, the monitor current) was read on a galvanometer. The length of the circular arc from entrance window *A* to the opening of the faraday cage was 12.02 cm. The amount by which the actual path length of the protons differed from this, owing to edge effects of the magnetic field, will be discussed later. Can *J*, projecting into the chamber, allowed a synchronous-motor-driven fluxmeter to be introduced between the pole faces.

The foregoing arrangement provided a magnetic analyzer for measuring beam energies after the entrance window, and it was so used in the experiment. The magnetic field was exactly zeroed, as indicated by the fluxmeter, and the electromagnet current then gave a measure of the momentum of the protons. A calibration was carried out by removing window *A* and tabulating magnet currents and corresponding beam energies, the latter being measured by means of a cylindrical electrostatic analyzer.<sup>13</sup>

In addition to the charged beam a neutral component, indicated by the straight dotted line, emerged from window *A* because capture processes take place in the

<sup>12</sup> See reference 3, p. 1028.

<sup>13</sup> S. K. Allison *et al.*, Rev. Sci. Instr. 20, 735 (1949).

window material. Another effect arising from the window was elastic scattering of the proton beam. Although the faraday cage in detector  $D_1$  could be expected to be insensitive to neutral atoms, those formed by capture processes in the scattered beam were prevented from entering the detector by means of baffle  $B$ . This baffle intercepted most of the scattered particles which could give rise to neutral atoms entering the 60-degree detector  $D_1$ .

Detector  $D_2$  was used in measuring the equilibrium attenuation ratios  $\rho_e$ , as will be described later. Figure 2 shows the cross section of a detector.

### 3. The Vacuum System

The electron exchange chamber could be evacuated or filled with hydrogen at the low operating pressures used in the experiment (of the order of  $10^{-2}$  mm Hg) through manifold  $G$ . In the following discussion needle valve  $NV_1$  may be assumed to be closed. With valve  $V_1$  open the high vacuum obtained was about  $4 \times 10^{-5}$  mm Hg. Upon closing this valve, the rate of rise of pressure, in the absence of hydrogen, never exceeded  $2 \times 10^{-3}$  mm Hg per hour, corresponding to a leak rate of about  $4 \times 10^{-3}$  cc per hour. Since the time lapses between successively pumping out the system did not exceed ten minutes, this leak rate was negligible.

With valve  $V_1$  closed, hydrogen from a palladium leak could be admitted to the system through valve  $V_3$ . Pressures were measured by means of a McLeod gauge, connecting through valve  $V_4$ .

An additional diffusion pump was attached through line  $L$  to the collimating tube. Valve  $V_2$  was provided in order to equalize the pressures on both sides of window  $A$  while the system was pumped down and was closed when a high vacuum was obtained.

### B. Experimental Arrangement for Measuring the Equilibrium Attenuation Ratios

In making these measurements it was desirable to have as nearly pure a proton beam as practicable and hence to eliminate the excessive neutral component arising from capture processes in window  $A$ . Therefore, the window was replaced by a small brass diaphragm  $K$  with a 0.51-mm diameter hole (No. 76 drill), having a sharply beveled edge, as shown in the detail drawing at the bottom of Fig. 1. Since the individual wires of the monitoring screen  $H$  could cover an appreciable fraction of the area of such a hole, the screen was replaced by a thimble  $T$ , separated by a Lucite spacer  $S$  from diaphragm  $C_2$ . The hole in the end of  $T$  had a diameter of 1.19 mm and, therefore, intercepted a portion of the collimated beam, passing the rest to diaphragm  $K$ .

The diffusion pump on line  $L$  evacuated the space behind diaphragm  $K$  and thus provided differential pumping to isolate the exchange chamber from the high vacuum of the beam-defining tube. The pressure in the exchange chamber was maintained at the desired

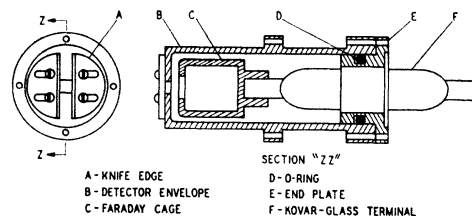


FIG. 2. Cross section of faraday-cage detector.

magnitudes by matching the rate of flow of hydrogen into the exchange chamber with the effusion rate through the hole in diaphragm  $K$ . Needle valve  $NV_1$ , leading back to the diffusion pump, provided a fine adjustment on the rate of flow of hydrogen into the chamber.

The proton beam in this part of the experiment was collected by the faraday cage of detector  $D_2$  whose slits were opened to 3.5 mm.

## III. EXPERIMENTAL PROCEDURE

### A. The Electron Capture Cross Sections

#### 1. Procedure Used in Obtaining the Data

The energy of the ion beam was set; and with the exchange chamber evacuated, a "profile" of the current to the 60-degree detector *versus* magnet current was obtained. As always, the magnetic field was carefully adjusted to zero by means of the fluxmeter before beginning, and the magnet current was increased throughout the desired range, with no decreases to give hysteresis errors. The profiles had widths at half-maximum of from 8 to 14 percent, a large fraction of which could be attributed to elastic scattering in the entrance window rather than to inhomogeneity of the beam energy. For convenience in obtaining protons at the lower energies, the molecular beam from the kevatron was often used; the molecules were dissociated in the window, giving protons of half the molecular beam's energy.

Having determined the beam energy from the peak of the profile, the magnet current was set at peak value and maintained at this value during the course of the run. The magnet coils and their series rheostats were water-cooled, so that there was very little drift of the magnet current, and only slight adjustments were required during a run to compensate small fluctuations in the voltage of the motor-generator set supplying the coils. Both magnet current and accelerator voltage were held constant to within less than one percent during the runs.

With the beam thus held in position on the 60-degree detector the ratio  $r(0)$  of the detector-galvanometer deflection to the monitor-galvanometer deflection was measured with the electron-exchange chamber evacuated to less than  $10^{-4}$  mm Hg. Hydrogen was admitted to the chamber, during which process the detector

TABLE I. Relative detector currents at various hydrogen pressures for a 44.5-keV proton beam and the calculation of the electron-capture cross section from these data.

Hydrogen pressure $p$ 10 <sup>-2</sup> mm Hg	Normalized detector current $r$	Attenuation ratio $\rho(p) = r(p)/\text{mean } r(0)$
<0.01	0.636	
0.97	0.322	0.322/0.630=0.511
<0.01	0.624	
1.61	0.199	0.199/0.167=0.322
<0.01	0.611	
0.75	0.339	0.339/0.595=0.570
<0.01	0.580	

Calculation of the capture cross section:

$$s = \text{slope of straight line in Fig. 3} = 30.9 \pm 0.9 \text{ (mm Hg)}^{-1}$$

$$T = \text{room temperature} = 294.7^\circ\text{K},$$

$$\sigma_c' = \text{uncorrected capture cross section} = 2.959 \times 10^{-18} s (T/298) \\ = (9.04 \pm 0.27) \times 10^{-17} \text{ cm}^2,$$

$$\sigma_c = \text{corrected cross section} = \sigma_c' + \sigma_g = \sigma_c' + 0.108 \times 10^{-17} \\ = (9.15 \pm 0.27) \times 10^{-17} \text{ cm}^2.$$

current decreased; and when a suitable pressure had been reached, the flow was stopped. The ratio  $r(p)$ , at hydrogen pressure  $p$ , was then determined, and the hydrogen pressure was measured with the McLeod gauge. Finally, the chamber was evacuated and the ratio  $r(0)$  measured again. The cycle was then repeated for a different pressure.

It should be emphasized that since only ratios of the currents were required, the absolute values were not important in the cross-section measurements. These values were, however, a few thousandths of a microampere. The linearity of the amplifier-galvanometer

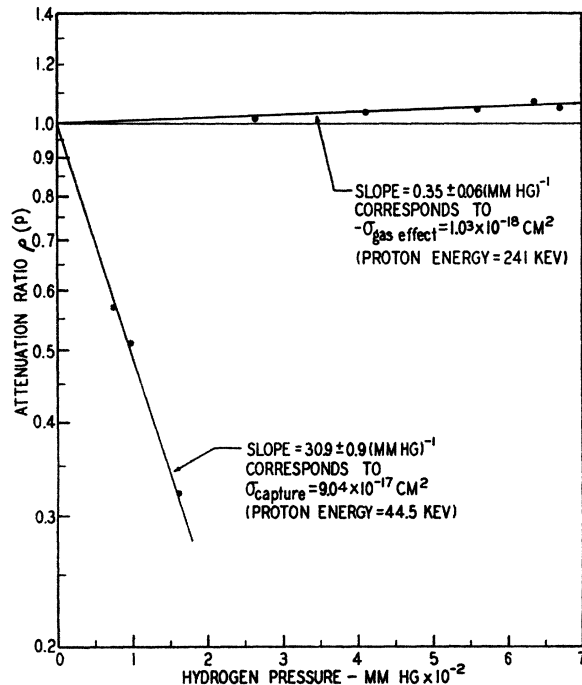


FIG. 3. Lower curve: Attenuation curve for a 44.5-keV proton beam at the 60-degree detector. Upper curve: Variation of detector response with hydrogen pressure.

arrangements (exclusive of input resistors) was checked over the operating range and found to be good to better than one percent.

In measuring the ratios  $r(0)$  and  $r(p)$ , three or more readings were taken and averaged; and in each run a minimum of two, and usually three or four, pressures were used. In terms of these ratios the attenuation ratio  $\rho(p)$  of Eq. (1) is given by

$$\rho(p) = r(p)/r(0). \quad (3)$$

The data for a typical run at a beam energy of 44.5 keV are given in Table I and plotted in Fig. 3 (lower curve). Using  $d = 12.02$  cm, Eq. (1) gives for the electron-capture cross section per atom,

$$\sigma_c = 2.959 \times 10^{-18} s (T/298), \quad (4)$$

where  $s$  is the slope of the line ("attenuation curve") in Fig. 3, expressed in  $(\text{mm Hg})^{-1}$ , and  $T$  is the absolute temperature. In the sample calculation of Table I the value of  $\sigma_c$  derived from the slope of the attenuation curve is called  $\sigma_c'$ . It is necessary to correct this value by adding a small quantity  $-\sigma_g$  due to the effect of gas on the detector, as will presently be explained, to obtain the value  $\sigma_c$  of the electron capture cross section.

## 2. Tests for Experimental Errors

When the faraday cage was used in measuring proton current in this part of the experiment, it was always situated in a strong magnetic field, which varied from about 1900 to 5500 gauss for the energy range of protons used. Therefore, it was not necessary to bias the cage in order to trap completely all secondary electrons produced by the proton beam in the cage. In order to check this point, the voltage from a well-insulated battery was applied between the grid of the beam-current amplifier and the faraday cage of the 60-degree detector (faraday cage positive). With proton beams of 61 and 258 keV and the exchange chamber evacuated, no difference was observed in the detector-galvanometer deflections for the conditions of zero and 100 volts on the faraday cage. Thus, it can safely be assumed that the cage did not respond to neutral atoms whose effect would be to produce secondary electrons from the surfaces which they struck. Therefore, no correction of the path length, owing to the entry of neutral-hydrogen beam atoms from positions at small distances in front of the detector, was applied. Neither were neutral atoms arising from capture processes in the proton beam scattered by the entrance window registered. A large fraction of these were excluded by means of baffle  $B$  of Fig. 1 whose knife edge was separated from the center of the bent beam by about 2 mm.

However, with a beam entering the faraday cage, the response of the detector itself was found to be somewhat affected by the presence of hydrogen gas. In order to measure this effect the beam energy was set at a value sufficiently high (295 keV) that the effect of

electron capture (as given by  $\sigma_c'$ ) was certainly negligible. With the proton beam bent into the faraday cage at the 60-degree position, the normalized detector current rose by a few percent as the pressure of hydrogen was increased up to the maximum value (about  $7 \times 10^{-2}$  mm) used in the experiment. The percent rise was also found to be independent of beam current. At slightly lower energies where there was some residual capture cross section, this rise decreased. However, by using the values of  $\sigma_c'$  extrapolated from the working energy region (32 to 150 keV), it was possible to correct for this. When this was done, the rise was found to be independent of beam energy within experimental error. The data for a typical rise corresponding to a beam energy of 241 keV are plotted in Fig. 3 (upper curve). Such a rise can be represented by an equivalent negative cross section.

In order to estimate the effect at lower energies where capture processes caused a large attenuation of the bent beam, the 60-degree detector was inserted at the zero-degree position, and a 0.025-mg/cm<sup>2</sup> aluminized zapon foil was placed about 3 mm in front of the detector. Capture and loss processes occurring in the gas of the chamber did not affect the faraday cage current, since the beam emerging from the foil covering the cage had an equilibrium distribution of protons and atoms, regardless of the composition of the beam impinging on the foil. With a magnetic field of about 100 gauss it was possible to prevent secondary electrons ejected from the foil from entering the cage and still to work on the portion of the beam scattered slightly by the entrance window. Measurements at 109 and 137 keV gave gas effects which were of the same size as those obtained before, indicating that the effect was independent of energy and magnetic field.

Table II gives the data for the gas effect. In the second column are the equivalent negative cross sections corresponding to the slopes of the gas-effect rises. Column 3 gives the extrapolated values of  $\sigma_c'$  added to their magnitudes to correct them, and the last column gives the gas effect  $-\sigma_g$  itself. It can be represented as a constant correction to be added to the cross sections  $\sigma_c'$ , giving for the corrected capture cross section:

$$\sigma_c = \sigma_c' + \sigma_g. \quad (5)$$

Such an effect was also observed by Montague,<sup>14</sup> who used a different type of detector in his measurements of loss cross sections and attributed the effect to ionization produced by the beam in the detector. In the present case the correction is somewhat smaller, but it is difficult to see how it is produced by ionization in view of the geometry of the detector. It should perhaps be mentioned that the voltage developed by the beam current across the input resistor to the beam-current amplifier (100 megohms) never exceeded 0.11 volt.

## B. The Equilibrium Attenuation Ratios

### 1. Procedure Used in Obtaining the Equilibrium Data

Since there was no entrance window in this case, the proton beam was well defined, and the profiles were quite narrow. Therefore, the beam energy was measured simply by visually observing the peak of the 60-degree detector currents.

With the beam energy held constant, the field was carefully zeroed and then increased to a value of about 60 gauss in order to trap secondary electrons in the faraday cage. The slits of the zero-degree detector were set sufficiently wide that the beam still entered the faraday cage at this weak field. Hydrogen pressure was then allowed to build up in the exchange chamber, and needle valve  $NV_1$  of Fig. 1 was adjusted so that the pressure remained approximately constant at the desired value. The ratio  $r(p)$  of detector- and monitor-galvanometer deflections was then read, the flow of hydrogen was stopped, and the system was pumped to high vacuum. Finally, the ratio  $r(0)$  was determined.

TABLE II. Effect of hydrogen gas on detector response, expressed as an equivalent negative cross section.

Proton energy keV	Negative cross section corresponding to gas effect $\text{cm}^2 \times 10^{-18}$	Extrapolated capture cross section $\sigma_c' \text{ cm}^2 \times 10^{-18}$	Corrected gas effect $-\sigma_g \text{ cm}^2 \times 10^{-18}$
295	$1.07 \pm 0.06$	0	$1.07 \pm 0.06$
241	$1.03 \pm 0.18$	0.033	$1.06 \pm 0.18$
208	$0.94 \pm 0.42$	0.10	$1.04 \pm 0.42$
190	$0.86 \pm 0.17$	0.25	$1.11 \pm 0.17$
137	$1.10 \pm 0.28$	...	$1.10 \pm 0.28$
109	$0.84 \pm 0.16$	...	$0.84 \pm 0.16$

Equivalent gas-effect cross section used in correcting the data:  
 $-\sigma_g = (1.08 \pm 0.10) \times 10^{-18} \text{ cm}^2.$

The process was repeated for a number of hydrogen pressures. As pressure increased, the attenuation ratio  $\rho(p)$  at first decreased and then reached an approximately constant value. A slight rise at saturation occurred because of the gas effect discussed in the last section, and the data were corrected for this effect. In taking each point, the ratio  $r(p)$  was read quickly in order to minimize fluctuations in pressure, and gas was trapped in the McLeod-gauge bulb at the time of reading the galvanometer deflections.

Three such runs were made at energies of 59.0, 66.7, and 73.0 keV. In order to obtain decreases in attenuation ratio which were sufficiently large for its accurate determination, it was necessary to run at low energies where  $\sigma_i/\sigma_c$  is close to unity. However, since there was no entrance window, dissociated molecules could not be used to furnish low energy protons, and the lowest proton energy used was, therefore, that for which the beam from the kevatron focused sufficiently well to give a workable beam.

The data are plotted in Fig. 4 with the equilibrium value,  $\rho_e$ , of  $\rho(p)$  indicated for each curve. It can be

<sup>14</sup> See reference 3, p. 1031.

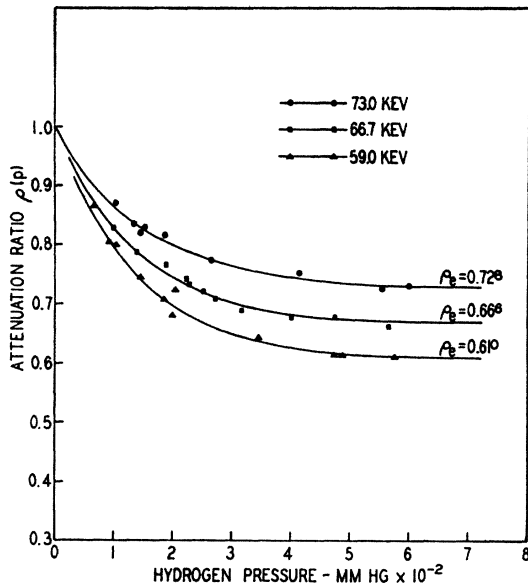


FIG. 4. Attenuation curve, showing the attainment of charge equilibrium, for mixed neutral-atom and proton beams at the zero-degree detector.

shown<sup>15</sup> that these curves should be of the form

$$\rho(p) = \rho_e + (1 - \rho_e) \exp[-(\sigma_i + \sigma_c)n(p)d'], \quad (6)$$

where  $d'$  is the distance between the entrance to the exchange chamber and the zero-degree detector. The curves shown in Fig. 4 were obtained by using this form to fit the data. It may be noted that this equation allows a determination of  $(\sigma_i + \sigma_c)$ ; however, no attempt was made to determine this quantity accurately from these data, since instabilities in pressure did not allow an accuracy comparable to that obtained for the cross sections themselves. Such small variations in pressure did not affect the accuracy of the determination of  $\rho_e$ , however.

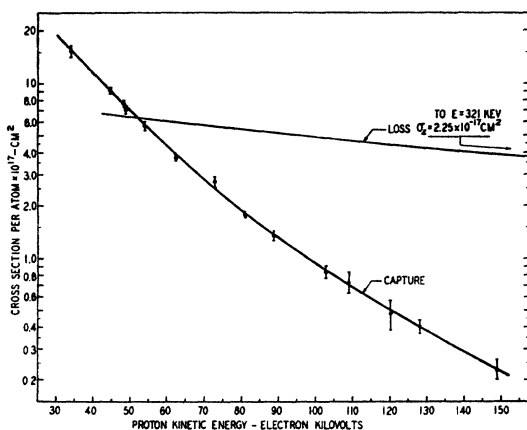


FIG. 5. Electron capture and loss cross sections as functions of ion energy for hydrogen beams in hydrogen gas.

<sup>15</sup> See reference 2, p. 507.

## 2. Tests for Experimental Errors

It was further verified that the faraday cage at the zero-degree position in these runs did not respond to a neutral beam. With chamber evacuated and sufficient magnetic field to deflect away the protons, no detector-galvanometer deflection was observed when the entrance hole was replaced by an aluminized zapon window which gave a neutral component of beam entering the cage.

An attempt was made to see if the presence of hydrogen gas caused a broadening of the beam as measured at the 60-degree detector. With the 0.5-mm entrance hole and the detector slit set at 1.06 mm, profiles were taken with and without gas in the chamber. No increase due to the presence of hydrogen was observed in the half-width for a pressure of about  $3 \times 10^{-2}$  mm Hg pressure, at a beam energy of 60 keV. This indicated that scattering by the gas in the chamber was negligible.

## IV. RESULTS

### A. The Electron Capture Cross Sections and the Ratio $\sigma_i/\sigma_c$

The results of the measurements of electron-capture cross sections are summarized in Fig. 5 in which  $\sigma_c$  is plotted as a function of energy. For comparison, the results obtained by Montague<sup>3</sup> in this energy range for the electron-loss section  $\sigma_e$  are also plotted in this graph.

The values of  $\sigma_e$  are tabulated in the second column of Table III; in the third column are the values of  $\sigma_i/\sigma_c$  obtained by dividing the magnitudes of the loss cross sections measured by Montague by those of the capture cross sections obtained here. This ratio is plotted as a function of energy in Fig. 6 (the curve marked M & R).

### B. Consistency of the Measurements of $\sigma_i$ and $\sigma_c$

The consistency of the measurements of the two cross sections, at least in the range of energies in which the equilibrium ratio  $\rho_e$  was measured, is indicated by the graph in Fig. 7. In the upper curve the values of  $\rho_e$  given in Fig. 4 are plotted as a function of energy. The lower curve is a plot of  $\rho_e$  derived from Eq. (2), using the values  $\sigma_i/\sigma_c$  obtained from Fig. 6. The discrepancy between the two results can be attributed to a small component of neutral atoms in the incident beam of the equilibrium-ratio experiment which arose from capture and loss processes taking place on the periphery of the entrance hole to the exchange chamber and in the residual gas in the beam-defining tube. If one assumes a fraction  $\nu$  of neutral atoms in the incident beam, Eq. (2) should be modified to read

$$\rho_e = (\sigma_i/\sigma_c) / [(1 - \nu)(1 + \sigma_i/\sigma_c)]. \quad (2')$$

Solving this equation for  $\nu$ , using the values of  $\rho_e$  and  $\sigma_i/\sigma_c$  corresponding to 59.0, 66.7, and 73.0 keV, gives, respectively, 4.5, 2.4, and 4.2 percent. These values are about what might be expected from edge effects.

An attempt was made to estimate the neutral component using a secondary-emission detector described by Montague.<sup>16</sup> Measurements made by comparing the responses of this detector (at the zero-degree position) to the total beam and to the neutral beam, when the protons were deflected away by the magnetic field, indicated a small neutral component. However, the relative responses of the detector to neutral and charged particles, as well as the dependence of its multiplication on magnetic field, were not known and could not be determined without further, rather extensive, experiments.

The measurements of  $\rho_e$  provide estimates of  $\sigma_l/\sigma_c$ . From the foregoing it is concluded that the values derived from the separate measurements of  $\sigma_l$  and  $\sigma_c$  are consistent with the direct estimates of their ratio to within 10 percent.

TABLE III. The electron-capture cross sections  $\sigma_e$  and the ratio,  $\sigma_l/\sigma_e$ , of loss and capture cross sections for hydrogen beams passing through hydrogen gas.

Hydrogen-beam energy $E$ kev	Electron-capture cross section per atom $\sigma_e$ $10^{-17}$ cm <sup>2</sup>	Ratio of loss and capture cross section $\sigma_l/\sigma_e$
34.0	15.2 ± 0.85	...
44.5	9.15 ± 0.27	0.728
48.3	7.65 ± 0.21	0.851
48.7	7.05 ± 0.16	0.922
53.9	5.73 ± 0.51	1.10
62.5	3.76 ± 0.11	1.61
72.9	2.75 ± 0.29	2.07
81.1	1.77 ± 0.02	3.09
88.8	1.36 ± 0.17	3.86
103	0.842 ± 0.069	5.79
109	0.733 ± 0.017	6.41
120	0.485 ± 0.098	9.20
128	0.410 ± 0.033	10.5
149	0.229 ± 0.028	17.1

### C. Accuracy of the Measurements

The limits of random error in the measurements of  $\sigma_e$  are given in Table III and indicated on the experimental points of Fig. 5. They were estimated from the spread of points about the attenuation curves and thus take into account instrument-reading errors and fluctuations in the experimental conditions. In addition, there were systematic errors which are enumerated below.

#### 1. The Effect of Gas on the Detector Response

Values of  $\sigma_e$  are given for energies up to the maximum at which measurements were made of 149 kev. At this end of the energy range, however, the capture cross sections have small magnitudes, comparable with the correction  $-\sigma_g$  due to the detector gas effect. This correction rapidly becomes less important at lower energies and represents only 0.71 percent at the lowest energy (34 kev) used. The systematic error in capture cross

<sup>16</sup> See reference 3, p. 1029.

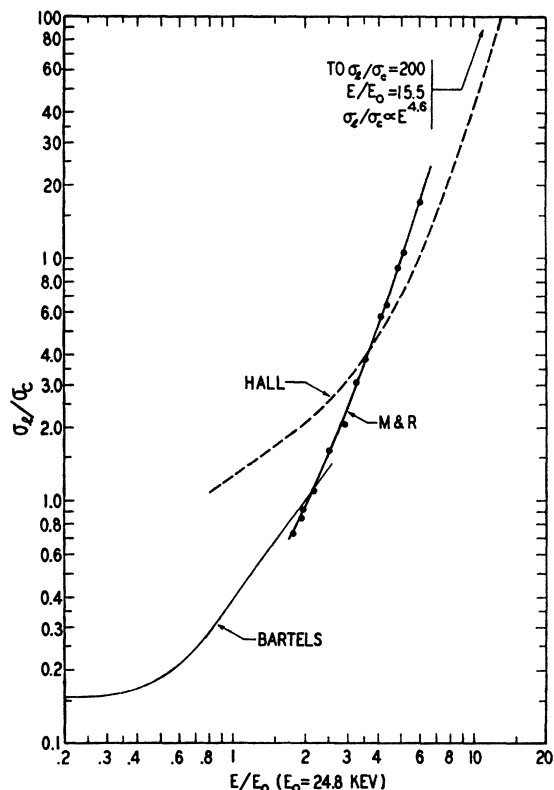


FIG. 6. Ratio of loss to capture cross section  $\sigma_l/\sigma_e$  as a function of ion energy  $E$ . Curve M & R and that of Bartels: Hydrogen beams in hydrogen gas. Curve of Hall: Hydrogen beams in the metals Be, Al, and Ag.

section due to this correction is estimated to be 0.07 and 5 percent at the lower and upper energy extremes of the measurements, respectively.

#### 2. Inhomogeneity of the Beam Energy

Some inhomogeneity was introduced into the beam energy by straggling arising from energy loss in the

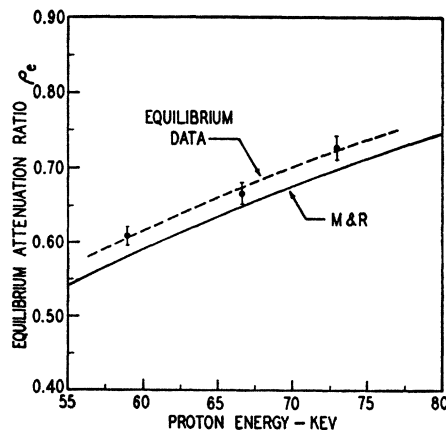


FIG. 7. Comparison of the equilibrium attenuation ratios  $\rho_e$  derived from the separate measurements of  $\sigma_l$  and  $\sigma_e$  (the curve marked M & R) with those measured directly.

entrance window to the electron-exchange chamber.<sup>17</sup> For an energy loss of 6.5 kev this straggling is estimated to be about 0.9 percent of the beam energy at the lowest value (34 kev) used. In addition, the ripple of the kevatron voltage gave rise to an energy inhomogeneity. Morrish<sup>18</sup> has measured the effect for this accelerator. Assuming a total current drain of 400 microamperes in the present experiment, his results yield an energy spread of about 3.0 percent due to ripple at a beam energy of 34 kev.

It should be noted that the proton beam in the measurements of  $\sigma_c$  was held accurately on the 60-degree detector by means of the magnetic field. With this arrangement the proton energy was selected to within a total spread of 1.8 percent. Any systematic correction of the capture cross-section curves arising from inhomogeneity of the beam energy is thus considered negligible.

### 3. Determination of the Path Length for Electron Capture

Since there was some fringing of the magnetic field, the path of the protons was not precisely circular as indicated in Fig. 1. In order to determine the amount by which the path length  $d$  varied from the circular-arc length of 12.02 cm, the variation of the magnetic field along the nominal circular path was measured throughout most of its 60-degree extension. Using a search coil of 1-cm diameter on the generating fluxmeter, the field was found to be weakened by respectively 9 and 26 percent at the entrance and detector ends of this circular arc and to be homogeneous to within 1 percent over 60 percent of this arc. The difference in fringing at the ends of the arc was due to the magnetic shielding about the entrance window.

Since the ends of the protons' path were fixed at the positions of the entrance window and of the detector, the main effect of this field inhomogeneity was merely to require a larger field at the center of the exchange chamber for bending protons of a given energy than would have been necessary had the field been uniform. A first-order calculation which took account of the variation of curvature of the proton orbit showed that the path length was increased by considerably less than 1 percent; although the "field strengthening" was about 2 percent. Thus, the correction to be added to the value 12.02 cm of  $d$  was negligible.

### 4. Elastic Scattering in the Hydrogen Gas

Appreciable scattering by the nuclei of the gas in the exchange chamber would have caused the capture cross sections to appear too large. That this effect was negligible, however, was indicated by the fact that no broadening was observed in a well-collimated beam at

the 60-degree detector. In addition, since the beam in the measurements of  $\sigma_c$  was spread by elastic scattering in the entrance window to a width considerably greater than that of the detector slit, the "geometry" was poor for observing such scattering in the gas. Bartels,<sup>5</sup> using good collimation and thicknesses of hydrogen gas comparable to those used here, observed no elastic scattering of protons at 30 kev. If there were such an effect in the present experiment, it would be included in the measured detector gas-effect correction  $-\sigma_g$ .

### 5. McLeod-Gauge Calibration

The McLeod gauge was calibrated by measuring the volume of its bulb and the diameter of its capillary. The consistency of several measurements indicated a calibration error of less than 1 percent.

## V. DISCUSSION

### A. The Capture Cross Section

From Fig. 5 it is seen that the capture cross section varies much more rapidly with energy than does the loss section. A log-log plot of the data shows that  $\sigma_c$  varies approximately as  $E^{-3.5}$  at the upper end of the energy range (100 to 150 kev), while the value of the exponent reported by Montague for  $\sigma_l$  in the region 120 to 329 kev is  $-0.70$ . This difference is qualitatively in accord with previous observations and theory. Rutherford<sup>19</sup> obtained the value  $-2.8$  for this exponent for the capture by doubly-charged alpha-particles in air and the value  $-0.5$  for the corresponding loss cross section. Brinkmann and Kramers,<sup>20</sup> using the first Born approximation, calculated the cross sections for capture into the Bohr orbits of a moving ion from hydrogen. Their result gives a variation of  $\sigma_c$  as  $E^{-6}$ , asymptotically for  $E \gg E_0$ , where  $E_0$  is the kinetic energy at which the ion velocity is equal to that of an electron in the first hydrogen Bohr orbit ( $v_0 = e^2/\hbar$ ). In the present experiment, however,  $E/E_0$  varies between 1.37 and 6.01, so that this condition is not met. A decrease in the numerical value of the exponent at lower energies is predicted, however; and it might be worth noting that the value of the exponent obtained from their equation in the energy range 100 to 150 kev is about  $-3.8$ .

The difference between the exponent  $-3.5$  observed in this experiment ( $1.17 \leq v/v_0 \leq 2.46$ ) and Rutherford's value of  $-2.8$  ( $4.1 \leq v/v_0 \leq 8.3$ ) indicates a more rapid decrease of  $\sigma_c$  with increasing ion velocity for hydrogen than for heavier stopping atoms. On classical grounds, Bohr<sup>21</sup> estimates the value  $-3$  for this exponent for heavy stopping atoms. This difference in exponents for light and heavy stopping materials is in qualitative accord with the Brinkmann-Kramers result, which indi-

<sup>19</sup> E. Rutherford, *Phil. Mag.* **47**, 277 (1924).

<sup>17</sup> In his measurements of  $\sigma_l$  Montague (reference 3, p. 1033) overestimated this straggling in setting 45 kev as the lowest beam energy at which his results could be considered reliable.

<sup>18</sup> A. H. Morrish, *Phys. Rev.* **76**, 1651 (1949).

<sup>20</sup> H. C. Brinkmann and H. A. Kramers, *Proc. Akad. Amsterdam* **33**, 973 (1930).

<sup>21</sup> N. Bohr, *Kgl. Danske Videnskab. Selskab, Mat.-fys. Medd.* **18**, 115 (1948).



cates a decrease in the numerical value of the negative exponent, at a given velocity, with increasing atomic number of the stopping material.

Keene<sup>22</sup> has published a summary of the previous measurements of  $\sigma_c$  for protons in hydrogen gas. Of these measurements those of that author, of Bartels, and of Meyer extend to sufficiently high energies for comparison with the present data. At low energies both Keene and Bartels observe a maximum of the curve  $\sigma_c(E)$  at about 7 kev, but they disagree appreciably on the magnitude of  $\sigma_c$ . The present data appear to agree quite well with those of Bartels, forming a reasonable extension of his curve, which is given for proton energies up to about 32 kev. The data of Meyer and the present data differ appreciably in the region about 32 kev, with the former showing a smaller exponent in the dependence of  $\sigma_c$  on  $E$ .

### B. The Ratio $\sigma_i/\sigma_c$

In Fig. 6 are plotted curves of the ratio  $\sigma_i/\sigma_c$  obtained from the present experiment and that of Montague and also from the data of Bartels.<sup>5</sup> The curve given by Hall<sup>23</sup> for protons in the metals Be, Al, and Ag is also plotted for comparison.

A striking fact that appears from the data for protons in metals is that  $\sigma_i/\sigma_c$  for a given energy is approximately independent of the atomic number of the stopping material. The ratio  $\sigma_i/\sigma_c$  has the value unity for a proton velocity  $v$  of about one Bohr unit ( $v/v_0=1$ ). Hall gives for this critical ratio the value 0.95. The present data, however, indicate a value 1.44 for this critical ratio; and this difference between the values obtained for metals and for hydrogen is confirmed by Bartels's data for protons in hydrogen gas given in Fig. 6.

In calculating the effective charge of moving ions it is assumed that roughly all electrons of velocities less than the speed of the ion are stripped off, since  $\sigma_i/\sigma_c$  increases rapidly from unity for  $v/v_0>1$ . In some of the calculations on the stopping of heavy ions in heavy

gases the value  $v/v_0\approx 1$  obtained from previous measurements has been a rough guide. On this basis the higher value 1.44 obtained here would result in a lower effective charge for ions moving in hydrogen.

### C. The Effect of Negative Hydrogen Ions

At the lower energies, there is a possibility of forming negative hydrogen ions (binding energy of second electron=0.71 ev) in the traversal of matter by hydrogen atoms and protons. The capture cross sections obtained in the present experiment would hardly be affected, however, since the cross section for capture of two electrons by a proton can safely be assumed negligible. In Montague's measurements of  $\sigma_i$ , however, there was a possibility not only of loss of the orbital electrons of the neutral atoms of the beam but also of capture of electrons to form negative ions.

In order to estimate the effect of negative ions the beam emerging from the aluminized entrance window was analyzed for such ions. At 35 kev, the fraction of negative ions was about 3 percent of the proton component, while at 90 kev none were observed to within an experimental error of about 0.1 percent. Fewer negative ions are expected to be formed in hydrogen gas than in a metal owing to the smaller density of electrons per atom in the former. Since the measurements of  $\sigma_i$  extended only down to 45 kev, it seems safe to neglect the effect of negative hydrogen ions in these measurements. At lower energies, such as those used by Bartels in his measurements of  $\sigma_i/\sigma_c$ , there may, however, be such an effect, so that his results would represent  $(\sigma_i/\sigma_c)+\sigma_c^*/\sigma_i^*$  instead of  $\sigma_i/\sigma_c$ , where the starred quantities refer to transitions involving negative hydrogen ions and neutral atoms.

The author wishes to express his thanks to Professor S. K. Allison for suggesting this problem and for extending the facilities of his laboratory for its execution and for his helpful advice. Thanks also are due Mr. H. Kanner and Mr. D. S. Bushnell for their aid in taking the data, and to Dr. J. H. Montague for helpful discussions. Grateful acknowledgment is also made of an AEC Predoctoral Fellowship granted the author.

<sup>22</sup> See reference 9, p. 385, Fig. 18.

<sup>23</sup> See reference 2, Fig. 3. The curve plotted in Fig. 6 is the solid curve given by Hall.